Intramolecular Quenching of Excited Singlet States in a Series of Fluorescamine-Derivatized Nitroxides

Sarah E. Herbelin and Neil V. Blough*

Department of Chemistry and Biochemistry University of Maryland College Park, Maryland 20742

Received: February 2, 1998; In Final Form: April 9, 1998

Steady-state and time-resolved absorption and fluorescence measurements were used to probe the mechanism(s) of excited singlet state quenching by stable nitroxyl radicals in a series of fluorescamine-derivatized nitroxides. Rate constants for intramolecular quenching (k_q) acquired from fluorescence lifetime measurements were very high, ranging from $\sim 0.3 \times 10^{10}$ s^{-1} to $\geq 5 \times 10^{10}$ s^{-1}, and showed little dependence on solvent polarity. The k_q's did not track the values of the Dexter and Förster spectral overlap integrals, thus indicating that energy transfer, through either mechanism, cannot account for the quenching. Quenching by electron transfer also appears unlikely, owing to the dependence of k_q on solvent polarity and the complete lack of radical ion generation in highly polar solvents. Time-resolved absorption measurements revealed the presence of a very weak transient centered at ~470 nm in the diamagnetic reference compounds that was not observed in the paramagnetic nitroxides; this transient was tentatively assigned to the excited triplet state of the fluorescamine moiety. The rapid singlet state quenching in this series of compounds thus appears to arise from enhanced internal conversion.

Introduction

The mechanisms by which excited singlet states of organic compounds are quenched by stable nitroxide radicals has been the subject of numerous studies over the last several decades.[1−5] Much of this past work has been directed at disentangling the relative contributions of electron exchange, energy transfer, and electron transfer to the quenching process.[1] The more recent use of fluorescence quenching by nitroxides to examine dynamical processes in biochemical systems[6−9] and as the basis of a method for the fluorimetric detection of radicals in condensed phases[10−17] has significantly heightened interest in these mechanisms and has highlighted the need to acquire additional information on the factors controlling the rates and distance-dependence of the quenching. This information is needed to identify the dominant quenching route(s) operating for a particular chomophore−nitroxide pair so that better optical radical sensors may be developed.[10−17]

Depending on the particular chromophore−nitroxide pair under examination, as many as four mechanisms could contribute to the singlet state quenching.[1] These mechanisms include electron exchange induced intersystem crossing (or internal conversion), energy transfer by electron exchange (Dexter mechanism), resonance energy transfer (Förster mechanism), and electron transfer. We previously reported the results of an extensive photophysical study on the intramolecular quenching of fluorescence in a series of covalently linked naphthalene−nitroxides.[1] On the basis of the very weak solvent dependence of the intramolecular quenching rate constants as well as on other factors, we concluded that the quenching arose primarily from an enhanced rate of intersystem crossing induced by electron exchange. However, a more diverse suite of compounds need to be examined under a variety of solution conditions in order to gain a better understanding of the factors controlling intramolecular quenching of excited states by nitroxides.

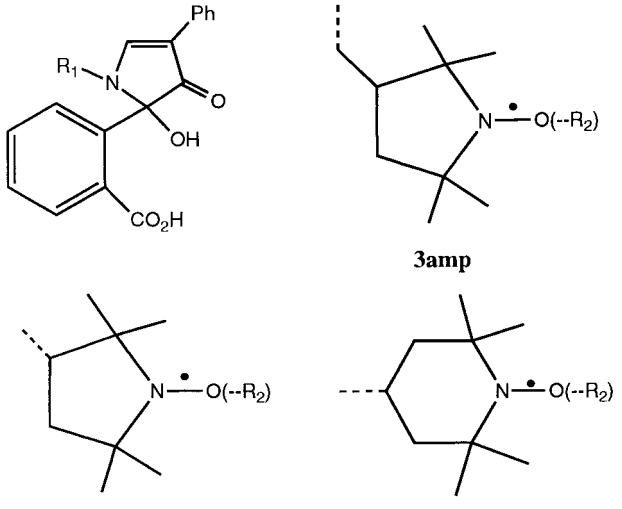

1a: R_1 = 3amp; R_2 = —, parent nitroxide
1b: R_1 = 3amp; R_2 = $COCH_3$
1c: R_1 = 3amp; R_2 = $CH(CH_3)_2$
2a: R_1 = 3ap; R_2 = —, parent nitroxide
2b: R_1 = 3ap; R_2 = $COCH_3$
3a: R_1 = 4at; R_2 = —, parent nitroxide
3b: R_1 = 4at; R_2 = $COCH_3$
3c: R_1 = 4at; R_2 = $CH(CH_3)_2$

Figure 1. Compounds examined in this study.

Here we extend our previous investigations to explore intramolecular singlet state quenching in a series of fluorescamine-derivatized nitroxides (Figure 1) by both time-resolved absorption and fluorescence measurements. Our choice of this

* To whom correspondence should be addressed at the Department of Chemistry and Biochemistry, University of Maryland, College Park, Maryland 20742. Fax: (301) 314-9121. E-mail: nb41@umail.umd.edu.

S1089-5647(98)00977-8 CCC: $15.00
Published on Web 05/22/1998

particular series was motivated not only by our interest in expanding the available data on intramolecular quenching by nitroxides but also by the recent use of these compounds as highly sensitive optical probes for detecting radicals produced in aqueous systems[11−15] and by cells.[16,17]

Experimental Section

Chemicals. Boric acid, sodium hydroxide, 4-amino-2,2,6,6-tetramethyl-1-piperidinyloxy free radical (4-at), 3-(aminomethyl)-2,2,5,5-tetramethyl-1-pyrrolidinyloxy free radical (3-amp), 4-hydroxy-2,2,6,6-tetramethyl-1-piperidinyloxy free radical (4-ht), and 3-carbamoyl-2,2,5,5-tetramethyl-1-pyrrolidinyloxy free radical (3-cp) were purchased from Aldrich. Distilled-in-glass grade diethyl ether was from Burdick & Jackson. 3-(Amino)-2,2,5,5-tetramethyl-1-pyrrolidinyloxy free radical (3-ap) was obtained from Kodak and 4-phenylspiro[furan-2(3*H*),1′-phthalan]-3,3′-dione (fluorescamine) from Sigma. High performance liquid chromatographic (HPLC) grade solvents were purchased from Aldrich or Sigma and used without further purification. Water used in all experiments was from a Millipore Milli-Q system. Standard buffer was 0.2 M borate, pH 8.1.

Preparation of Compounds. *Synthesis of **1a−3a**.* The syntheses of **1a-3a** employed procedures similar to those described by Bernardo et al.[18] for preparing the ethylamine derivative of fluorescamine. Equimolar amounts (∼1 mmol) of fluorescamine and the appropriate nitroxide, dissolved in 15 and 6.5 mL of acetonitrile, respectively, were combined and let sit for 15 min in the dark at room temperature. The reaction mixture was placed on ice and its volume slowly reduced to ∼5 mL by flushing with Ar and then stored overnight in a freezer at −20 °C. The resulting yellow precipitate was collected by centrifugation, dried under Ar, and then washed three times with 5 mL of diethyl ether.

Product purity was checked by HPLC using equipment and procedures described previously[11−14,17] employing an Applied Biosystems 785 absorption detector and a Hitachi F1050 fluorescence detector connected in series. The absorption detector was set to 390 nm (Figure 2), while the excitation and emission wavelengths of the fluorescence detector were set to 390 and 490 nm, respectively (Figure 2). Chromatograms acquired by absorption detection exhibited a major component corresponding to **1a−3a** (≥90%) and a minor component (≤10%) assigned tentatively to the lactone of **1a−3a**[18] based on the complete lack of fluorescence from this species.[18,19] In contrast, chromatograms acquired with fluorescence detection revealed a number of other components whose fluorescence was comparable in magnitude to that exhibited by **1a−3a**. These components, which represent minor contaminants with a high fluorescence quantum yield (and long fluorescence lifetime), did not seriously affect the time-resolved measurements because of their small contribution to the total decay amplitude. Thus, as expected, time-resolved fluorescence measurements of **1a−3a** by time-correlated photon counting showed a dominant short-lived component (92−98%; vide infra). Unfortunately, these minor contaminants did grossly interfere with the determination of fluorescence quantum yields.

Thus, to determine the quantum yields of **1a−3a,** these compounds were generated and purified by HPLC immediately prior to measurement. Approximately 4−9 mL of the appropriate aminonitroxide in standard buffer was derivatized with a 2-fold molar excess of fluorescamine (1−4 mL of 5 mM fluorescamine in acetonitrile) in Teflon vials. The reaction was carried out for 1 min at room temperature. The resulting fluorescamine-linked nitroxide was immediately purified by HPLC using procedures described elsewhere.[12−14] The purified compound, collected directly from the column, was immediately diluted into the appropriate solvent for the quantum yield measurement.

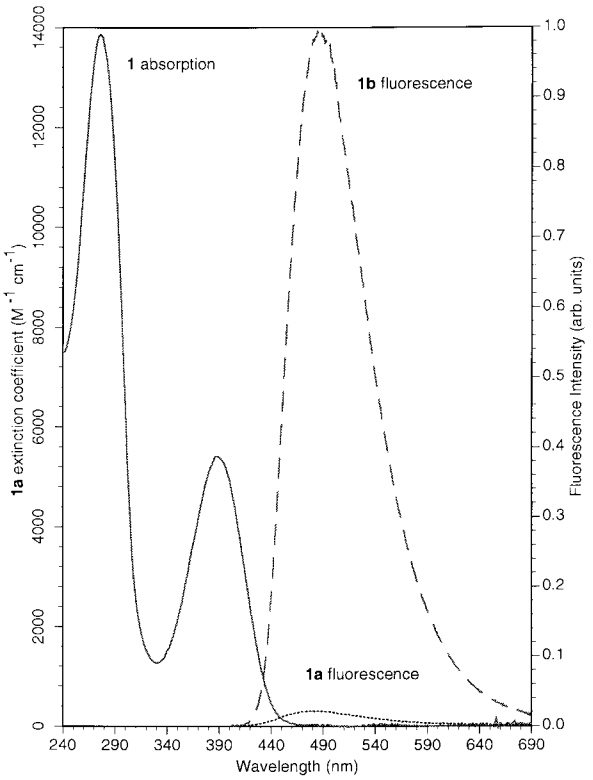

Figure 2. Absorption and fluorescence spectra of **1a** and **1b** in standard buffer (0.2 M borate, pH 8.1).

Synthesis of O-Alkylhydroxylamines. Compounds **1b,c**, **2b**, and **3b,c** were prepared and purified as described elsewhere.[12−14] The mass spectra of these compounds (as the lactones) were identical with those seen previously;[13,14] structures were confirmed by high-resolution mass spectrometry employing a VG Autospec Q and a desorption chemical ionization probe operated in the electron impact mode (50 keV): M^+ calcd for **1b** ($C_{28}H_{30}N_2O_5$) 474.2155, found 474.2143; M^+ calcd for **1c** ($C_{29}H_{34}N_2O_4$) 474.2518, found 474.2539; M^+ calcd for **2b** ($C_{27}H_{28}N_2O_5$) 460.1998, found 460.1988; M^+ calcd for **3b** ($C_{28}H_{30}N_2O_5$) 474.2155, found 474.2152; M^+ calcd for **3c** ($C_{29}H_{34}N_2O_4$) 474.2518, found 474.2520.

Optical Measurements. Absorption spectra were collected with a Hewlett-Packard 8451A diode array spectrophotometer (2 nm resolution), while fluorescence spectra were recorded with a SLM SPF-500C or a SLM AB2 spectrometer employing either 2/2 (**1b,c−3b,c**) or 4/4 (**1a−3a**) nm excitation/emission bandpasses. Absorption and fluorescence spectra of **1a−3a** were collected immediately after HPLC purification and the subsequent dilution of 1−100 μL of the compound contained in the HPLC mobile phase (64% methanol/36% pH 4.0 acetate buffer) into ∼3 mL of the appropriate solvent. **1b,c−3b,c** were dissolved in a small volume of dioxane (1−100 μL) and then diluted into ∼15 mL of the appropriate solvent. All spectra were recorded at room temperature. Quantum yields were determined relative to quinine sulfate as previously described.[1]

Time-Resolved Measurements. Solutions of **1a−3a** were prepared by dissolving a small quantity of the solid in solvent or by dilution in solvent immediately following synthesis as described above. Solutions of **1b,c−3b,c** were prepared in the same fashion as in the steady-state measurements. The absor-

TABLE 1: Spectral Characteristics of the Fluorescamine and Nitroxide Substituents

	fluorescamine substituent		absorption peak max, nm [extinction coefficient, $M^{-1}\,cm^{-1}$]		
solvent	singlet energy, eV	fluorescence peak max, nm	fluorescamine substitutent	3-cp[a]	4-ht[a]
buffer	2.82	492	386	398 [7.35]	430 [13.1]
acetonitrile	2.84	486	386	426 [5.58]	466 [9.95]
methanol	2.87	483	385	414 [6.83]	448 [10.7]
dioxane	2.86	485	384	430 [4.62]	468 [11.1]

[a] Because 3-ap, 3-amp, and 4-at were very hygroscopic, 3-cp and 4-ht were employed to obtain more accurate values for the extinction coefficients of the pyrrolidinyl and piperidinyl nitroxides, respectively.

bance of solutions prepared for fluorescence lifetime measurements were between 0.1 and 0.2 at 290 nm, while those for time-resolved absorption measurements were ~1 at the excitation wavelength (1 cm cell) as measured on a Hewlett-Packard 8450A diode array spectrophotometer.

Fluorescence lifetimes were measured by time-correlated single photon counting on an instrument at the Center for Fast Kinetics Research (Austin, TX). This system is described in detail elsewhere.[20] Briefly, excitation was provided by a cavity-dumped tunable dye laser, synchronously pumped with the second harmonic of a mode-locked Nd:YAG laser (Coherent, Antares). The dye pulses (6 ps fwhm, 1.8 MHz) were frequency doubled to 290 nm with a KDP crystal. Fluorescence was collected at 90° and focused into a monochromator tuned to 490 nm; entrance and exit slits were adjusted to obtain a counting rate of 4000−5000 photons per second impinging on the photomultiplier tube (PMT).

An Ortec 457 time-to-amplitude converter (TAC) received start pulses directly from the cavity dumper and stop pulses from the PMT. The TAC signal was passed to a multichannel analyzer and the data were saved in an IBM-compatible computer for analysis, storage, and hardcopy. The decay curves were fit to one to three exponentials with iterative deconvolution software based on algorithms developed by O'Connor[21] and written in ASYST language by Paul Snowden at CFKR. The instrumental response limit for this system is ~20 ps.

Time-resolved absorption measurements were performed with a conventional laser flash photolysis apparatus located in the laboratory of Dr. Daniel Falvey at the University of Maryland. This system employs a Questek 2120 excimer laser using Xe/HCl as the reagent gas for excitation at 308 nm. A 350-W xenon arc lamp, perpendicular to the path of the excitation source, served as the monitoring light source. Transient absorption signals were captured with a Lecroy 9420 350 MHz digital oscilloscope, and passed to an IBM clone for analysis. The instrumental response limit for this system is ~10 ns.

Energy Minimization of Molecular Structures. Energy-minimized molecular structures of **1a**−**3a** were acquired by using Nemesis 1.1, a molecular mechanics (MM2-type) program run under MicroSoft Windows GUI. The Nemesis program uses the computation and structure manipulation in chemistry (COSMIC) algorithm[22] to supply the force field for energy calculations and the conjugate gradient optimizer for structure optimization in energy calculations. COSMIC calculates molecular energies by summing the terms associated with bond length, bond angle, torsion angle, and van der Waals and Coulombic interactions, parametrized using tables of bending, stretching, and torsional force constants acquired experimentally. Minimization was considered complete when either the energy difference between successive iterations was less than 10^{-4} kcal/mol or the sum of the squares of the gradient vector components fell below 10^{-10} $kcal^2/mol^2/Å^2$. The structures of the molecular fragments (fluorescamine, 3-amp, 4-at, and 3-ap) were first entered into the program and then optimized by minimizing the electrostatic and van der Waals energies. Next, the appropriate radical, either 3-ap, 3-amp, or 4-at, was coupled to the fluorescamine moiety and the energy again minimized. To search for local minima, the bond(s) between the radical and fluorescamine moieties were rotated through 1−15° steps with a new molecular energy calculated at each step, thus providing a plot of molecular energy versus torsion angle. For **2a** and **3a**, rotation is only possible about the bond joining the nitroxide ring to the fluorescamine moiety ($N-R_1$ in Figure 1). For **1a**, two rotations are possible due to the presence of the methylene group. In this case, a 2-fold rotation was performed, thus producing a two-dimensional contour plot. Note that structures were not optimized at each rotation step.

From the energy-minimized structures of **1a**−**3a**, the fluorescamine-to-radical, nitrogen−nitrogen distance was calculated, as well as the angle between the planes of the five-membered ring of the fluorescamine moiety and the radical moiety. Ring planes were defined by the nitrogen atoms and their adjacent ring carbons. The angle between the ring planes was calculated from the atomic coordinates of the minimized structures by using a Matlab subroutine.

Results and Discussion

Absorption and Fluorescence Spectra. The absorption spectra of **1a**−**3a** were well described as a simple sum of the individual absorption contributions of the fluorescamine and nitroxide moieties (Figure 2, Table 1), as was observed previously for naphthalene−nitroxide adducts.[1] No new transitions potentially arising from strong electronic coupling between the fluorescamine and nitroxyl moieties were evident. The fluorescamine moiety exhibited absorption maxima at 272 and 392 nm and an emission maximum at ~488 nm (Figure 2); these maxima varied only weakly with solvent polarity (Table 1). The absorption maximum of the lowest energy band ($n \rightarrow \pi^*$) of the piperidinyl (4-ht or 4-at) and pyrrolidinyl (3-cp, 3-ap, or 3-amp) nitroxides was observed at 468 and 430 nm, respectively, in nonpolar solvents (dioxane), with the maximum of both undergoing blue shifts of ~30 nm with increasing solvent polarity (aqueous buffer). The possible impact of these energy differences and solvent-dependent blue shifts on intramolecular quenching is discussed below.

Although the fluorescence yields of the paramagnetic derivatives, **1a**−**3a,** were substantially smaller than those of the corresponding diamagnetic derivatives, **1b,c**−**3b,c** (vide infra), the emission line shape and wavelength maximum of the diamagnetic and paramagnetic compounds were identical and exhibited the same dependence on solvent polarity. These results indicate that the residual emission arising from **1a**−**3a** originates from the excited singlet state of the fluorescamine moiety, consistent with results obtained previously with other derivatives.[1]

Fluorescence Quantum Yields. Quantum yields for the paramagnetic derivatives, **1a**−**3a**, were substantially smaller than

TABLE 2: Quantum Yields of 1−3

compound	buffer	methanol	dioxane
1a	0.0013	0.00081	0.00066
1b	0.095	0.13	0.13
1c	0.085	0.14	0.17
2a	0.00046	0.00023	0.00050
2b	0.097	0.17	0.17
3a	0.015	0.045	0.0055
3b	0.060	0.18	0.21
3c	0.060	0.21	0.21

those of the corresponding diamagnetic *O*-alkylhydroxylamines, **1b,c**−**3b,c** (Table 2), ranging from 4-fold to several 100-fold lower. Larger differences in quantum yields were observed between the diamagnetic and paramagnetic derivatives of series **1** and **2** than for series **3**. The uncertainties in the quantum yield determinations for **1a** and **2a** are likely to be significant, due to the difficulty of measuring such low yields in the possible presence of variable amounts of highly fluorescent trace contaminants. Thus, it is not clear that the quantum yields for **1a** and **2a** differ significantly. However, the quantum yields for **3a** are clearly higher than those for **1a** and **2a**.

A previous study has shown that quantum yields for fluorescamine-derivatized amines fall between 0.09 and 0.34 with ethanol as the solvent[18] and our values for the diamagnetic species (**1b,c**−**3b**,**c**) are within this range. Within series **1** and **3,** quantum yields for the two types of O-alkylhydroxylamines (acetyl or isopropyl) were nearly identical in magnitude, demonstrating that substitution at this position does not influence the quantum yields significantly.

Lifetime Measurements and Intramolecular Quenching Rate Constants. The differences in quantum yields observed between the paramagnetic and diamagnetic compounds were also reflected in the fluorescence lifetimes (Table 3). The paramagnetic derivatives exhibited appreciably shorter fluorescence lifetimes than the diamagnetic compounds (Figure 3), in ratios nearly identical to those obtained for the quantum yields when corrections were made for diamagnetic impurities (Table 3). The fluorescence decays of **1a** and **2a** were dominated by a very short-lived component that was close to the time resolution of the instrument (∼20 ps); thus differences between these two compounds and their solvent dependencies could not be distinguished readily. When the fluorescence decays of **1a** and **2a** were acquired on longer time scales (50−90 ns), the lifetime of the minor, longer-lived component agreed closely with that of the corresponding diamagnetic compounds for a given solvent, suggesting the presence of a small percentage of diamagnetic contaminant.

In contrast to **1a** and **1b**, the fluorescence decay of **3a,** although short (Figure 3), was well above the time resolution of the instrument. However, the decay kinetics for **3a** were more complicated and best-fit as a sum of two short-lived components with lifetimes ranging from 42 to 120 ps and 0.22 to 1.3 ns, respectively (Table 3).

The fluorescence decay of the diamagnetic compounds in acetonitrile and buffer could be well-fit to a single exponential, whereas in dioxane, methanol, and cyclohexane, the decay was best-fit as a sum of two exponentials. The lifetimes obtained for the longer-lived component of the diamagnetic compounds in methanol (from 9.6 to 12.1 ns) and for the single component in aqueous buffer (from 2 to 4.6 ns) are longer than those found by DeBernardo et al.[18] for fluorescamine-derivatized butylamine (3.3 ns in methanol and 1.7 ns in water). However in methanol, the lifetimes of the shorter-lived component [1.6−3.3 ns (12−52%)] are consistent with their values. The diamagnetic

TABLE 3: Fluorescence Lifetimes of 1−3

	lifetime,[a] ns				
	buffer	acetonitrile	methanol	dioxane	cyclohexane
1a	0.029 (96%)[b]	≤0.020 (98%)[b]	≤0.020 (99%)[b]	0.031 (92%)[b]	*c*
1b	3.6 (100%)	12.1 (100%)	12.1 (62%), 2.2(38%)	11.1 (55%), 1.1 (45%)	9.3 (72%), 1.8 (28%)
1c	3.7 (100%)	12.2 (100%)	9.6 (55%), 1.6(45%)	11.3 (54%), 0.75 (46%)	9.9 (57%), 0.88 (43%)
2a	≤0.02 (96%)[b]	0.025 (91%)[b]	0.027 (76%), 0.39 (12%), 3.7 (12%)	0.029 (62%), 0.48 (22%), 23.4 (16%)	*c*
2b	4.6 (100%)	13.6 (100%)	11.9 (47%), 3.3 (53%)	12.1 (62%), 0.95 (38%)	11.1 (100%)
3a	0.12 (84%), 1.3 (16%)	0.059 (43%), 0.18 (57%)	0.054 (37%), 0.20 (59%)[b]	0.042 (43%), 0.22 (57%)	*c*
3b	1.99 (100%)	13.0 (100%)	11.5 (48%), 3.3 (52%)	11.7 (64%), 1.4 (36%)	9.3 (78%), 1.2 (22%)
3c	1.95 (100%)	13.5 (100%)	11.9 (71%), 1.7 (29%)	11.6 (55%), 0.80 (45%)	8.9 (51%), 2.0 (49%)

[a] Values in parentheses are the percent contribution of that lifetime component to the total decay amplitude. All χ^2 values were <6 for **1**−**3b** and **1**, **3c** and <3 for **1**−**3a;** most χ^2 values were ∼2. [b] Total is less than 100% due to diamagnetic impurities. [c] Insufficiently soluble to obtain a measurement.

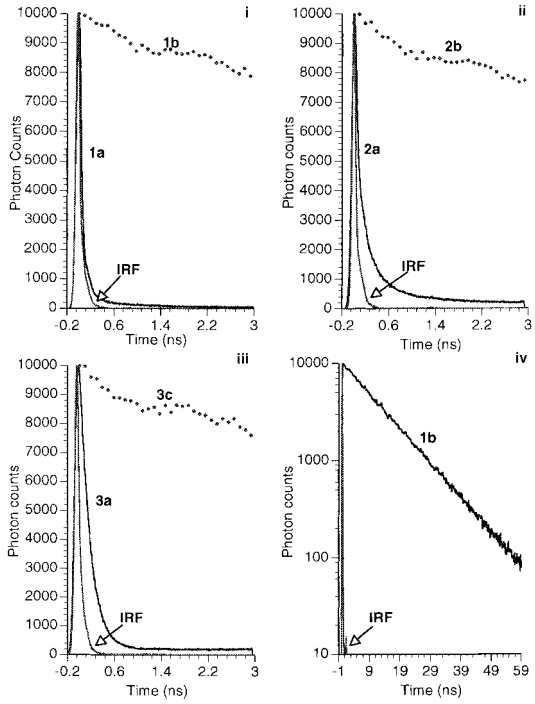

Figure 3. Fluorescence decays of the paramagnetic compounds (**1a**−**3a**) and corresponding diamagnetic analogues (**1b**, **2b**, **3c**) in acetonitrile along with the instrument response function (IRF). (i)−(iii) are on a linear scale and a 3 ns timebase, whereas (iv) is on a log scale and a 60 ns time base.

TABLE 4: Intramolecular Quenching Rate Constants, k_q ($\times 10^{-9}$ s^{-1})

compound	buffer	acetonitrile	methanol	dioxane
1a	34	≥50	≥50	32
2a	≥50	40	37[a]	34[a]
3a av[b]	3.2	7.8	7.3	7.0

[a] Multiexponential decay; calculated value based on the lifetime of the dominant short-lived component. [b] Multiexponential decay; average value calculated using eq 2 (see text).

compounds exhibited significantly shorter lifetimes (and lower quantum yields) in aqueous buffer as compared to the other solvents examined (Table 3). Consistent with the quantum yield measurements, the lifetimes for the different *O*-alkylhydroxylamines of a given series were very similar.

Intramolecular quenching rate constants, k_q, were calculated from the lifetime data obtained for the compounds in series **1** and **2** using the expression,[1]

$$k_q = \frac{1}{\tau_p} - \frac{1}{\tau_d} \tag{1}$$

where τ_p and τ_d are the lifetimes of the paramagnetic (p) and diamagnetic (d) derivatives, respectively, within a given series (Table 4). Because the lifetimes of the paramagnetic compounds in these series are so much shorter than the diamagnetic compounds, eq 1 effectively reduces to $k_q \sim 1/\tau_p$. In the case of series **3,** where two lifetimes were obtained for the paramagnetic compound, an average quenching rate constant, k_{qav}, was calculated by using the relationship[2]

$$k_{qav} = \frac{1}{(\tau_{p_1} c_{p_1} + \tau_{p_2} c_{p_2})} - \frac{1}{(\tau_{d_1} c_{d_1} + \tau_{d_2} c_{d_2})} \tag{2}$$

where c is the fraction of the total amplitude contributed by that component to the total fluorescence decay curve. Calculated values of k_q for **1a** and **2a**, ranging from $\sim 3 \times 10^{10}$ to $\geq 5 \times 10^{10}$ s^{-1}, were significantly greater than the values of k_{qav} calculated for **3a** ($\sim(3-8) \times 10^9$ s^{-1}) and exhibited only a weak dependence on solvent (Table 4).

TABLE 5: Parameters Calculated for the Ground State Geometry

compound	N−N distance, Å	angle[a]
1a	4.7	99.8°
2a	3.6	89.5°
3a	4.3	100.5°

[a] Angle between the plane of the five-membered ring of the fluorescamine moiety and the plane of the radical (Figure 1). Ring planes are defined in each moiety by the nitrogen atoms and the adjacent ring carbons.

Time-Resolved Absorption Measurements. Excitation at 308 nm of the diamagnetic compounds in a number of solvents gave rise to an extremely weak transient absorption signal centered at ~470 nm (data not shown). Because of the weakness of this signal, a reliable measurement of its lifetime could not be obtained, although it was evident that its lifetime was longer than the time resolution of the instrument. Excitation of the paramagnetic compounds in a number of solvents produced no signal that was clearly separable from the system noise.

Ground-State Geometry. Energy minimized N(nitroxide)−N(fluorescamine) distances decreased in the order **1a** > **3a** > **2a**, although the range in distances is not large (Table 5, Figure 1). The angle between the plane of the nitroxide moiety and the fluorescamine chromophore was close to 90° for all three compounds, implying that the π orbital of the nitroxide nitrogen is almost perpendicular to the π system of the five-membered ring of the fluorescamine moiety. A secondary minimum was found in each compound corresponding to an ~180° rotation about the fluorophore−nitroxide bond(s). The absence of large variations in N−N distances and ring plane angles suggests that all of the compounds have similar ground-state geometries. Interestingly, the presence of two well-resolved, short-lived fluorescence components in **3a** implies the existence of at least two conformers which are not interconverting on the time scale of the quenching and which differ significantly in their ability to quench the singlet. In contrast, **1a** and **2a** in buffer and acetonitrile exhibit only a single short-lived component, suggesting either the presence of a single, dominant conformer or multiple conformers whose differential ability to quench the singlet are small or cannot be resolved due to the rapidity of the quenching.

Quenching Mechanisms. As discussed previously,[1] a number of different mechanisms could account for the efficient excited singlet state quenching in these compounds. These mechanisms include Förster (dipole−dipole) and Dexter (electron exchange) energy transfer, electron transfer, and electron exchange induced intersystem crossing (or internal conversion). Förster and Dexter energy transfer rates are proportional to their overlap integrals, J_F and $J_{D,}$ respectively,[23]

$$J_F = \frac{\int_0^\infty F(\lambda)\epsilon(\lambda)\lambda^4 \, d\lambda}{\int_0^\infty F(\lambda) \, d\lambda} \tag{3}$$

$$J_D = \frac{\int_0^\infty F(\lambda)\epsilon(\lambda) \, d\lambda}{\int_0^\infty F(\lambda) \, d\lambda \int_0^\infty \epsilon(\lambda) \, d\lambda} \tag{4}$$

TABLE 6: Calculated Dexter and Förster Overlap Integrals

	J_D, cm			J_F, M^{-1} cm^3		
	buffer	methanol	dioxane	buffer	methanol	dioxane
1a	1.01×10^{-3}	2.18×10^{-3}	3.64×10^{-3}	3.58×10^{-18}	7.07×10^{-18}	8.96×10^{-18}
2a	1.08×10^{-3}	2.36×10^{-3}	3.74×10^{-3}	3.74×10^{-18}	7.50×10^{-18}	9.13×10^{-18}
3a	3.03×10^{-3}	4.71×10^{-3}	5.44×10^{-3}	2.37×10^{-17}	3.37×10^{-17}	4.23×10^{-17}

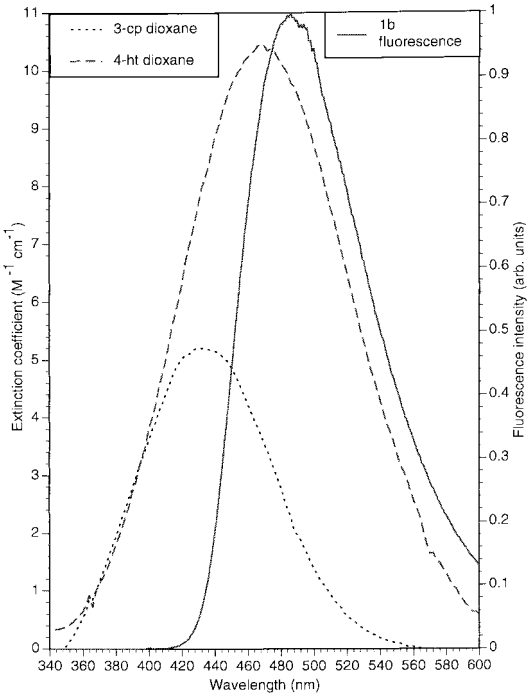

Figure 4. Absorption spectra of 3-cp and 4-ht in dioxane. The fluorescence emission spectrum of **1b** in standard buffer is included in order to illustrate the degree of spectral overlap between emission of the fluorescamine substituent and absorption by the pyrrolidinyl and piperidinyl nitroxide substituents.

where $F(\lambda)$ is the corrected fluorescence intensity of the fluorophore and $\epsilon(\lambda)$ is the extinction coefficient of the acceptor (nitroxide) at wavelength λ. Thus, larger values for the overlap integrals should lead to more efficient quenching and larger k_q's, if either the Förster or Dexter mechanisms were operational. However, although J_F and J_D are substantially larger for **3a** than for **1a** and **2a** (Table 6, Figure 4), the values of k_q are significantly smaller, directly contradicting the predicted trend. These differences are unlikely to be due to geometry as the calculated N−N distances and the angles between the radical and fluorophore planes are similar for all three compounds (Table 5). Furthermore, while the overlap integrals increase monotonically with decreasing solvent polarity due primarily to the large red-shift in the nitroxide absorption band (Table 1, Figure 4), the values of k_q do not show this same trend (Table 4).

Calculated Förster transfer rates are also inconsistent with energy transfer acting as a dominant quenching route. These rates were calculated using the expression[1]

$$k_{FT} = \frac{J_F \kappa^2 \phi_d}{R^6 \eta^4 \tau_d} 8.71 \times 10^{23} \qquad (5)$$

where κ^2 is the orientation factor (assumed to be $^2/_3$), ϕ_d and τ_d are the quantum yield (Table 2) and lifetime (Table 3), respectively, of the appropriate diamagnetic derivative, R is the donor−acceptor distance (Table 5), and η is the solvent refractive index. The resulting values of k_{FT} (Table 7) are much

TABLE 7: Calculated Förster Energy Transfer Rates, k_{FT} ($\times 10^{-9}$ s^{-1})

compound	buffer	methanol	dioxane
1a	1.5	1.5	1.6
2a	6.7	9.3	8.5
3a	24	19	20

smaller than the values of k_q observed for compounds **1a**, **2a** (Table 7; Table 4), although the values for **3a** are much closer. Sensitivity analysis shows that these values could be off by up to a factor of 5 if κ^2 is allowed vary from 0 to 4. However, because κ^2 approaches 0 as the angle between the plane of the donor and acceptor transition moments approaches 90°, the actual value is probably closer to 0 (Table 5). The absorption dipole for the nitroxide group is perpendicular to the NO bond, lying in the CNC plane, and is almost perpendicular to the transition moment of the fluorophore, which should lie in the plane of the five-membered ring of the fluorescamine moiety (Table 5). Thus we conclude that energy transfer, through either a Förster or Dexter mechanism, cannot account for the high rates of intramolecular quenching in these compounds.

Two pieces of evidence argue that electron transfer is also unlikely to act as the dominant quenching route in these compounds. First, time-resolved absorption measurements show no evidence of radical ion formation in the paramagnetic compounds, even in highly polar solvents. Second, the values of k_q show very little dependence on solvent polarity and, in one instance, appear to increase with decreasing solvent polarity (**3a**, Table 4), counter to what one would predict for electron transfer. Although electron transfer cannot be excluded unequivocally, we currently believe this quenching pathway to be unimportant based on this evidence.

The very weak absorption transient observed in the diamagnetic compounds is tentatively assigned to the excited triplet state of the fluorescamine moiety. Fluorescence quantum yields and lifetimes for the diamagnetic compounds are very similar to those of fluorescamine derivatives of simple alkylamines,[18] thus arguing that this transient does not result from an intramolecular electron-transfer process. The weakness of this signal implies either that the extinction coefficient for triplet−triplet absorption is very small in these compounds or, more likely, that the triplet is not extensively populated during singlet decay. The loss of this signal in the paramagnetic compounds suggests that singlet state quenching does not proceed through enhanced intersystem crossing but instead proceeds through the rapid parallel process of internal conversion. An alternative explanation is that the triplet is rapidly populated through enhanced intersystem crossing, but relaxation to the ground state occurs even more rapidly.[1] However, recent work[24,25] has shown that the rates of intramolecular triplet state quenching of aromatic hydrocarbons by nitroxides are slower than singlet state quenching by 2 orders of magnitude or more, thus making this latter pathway very unlikely. The rapid singlet state quenching observed in this current series of compounds thus appears to arise through enhanced internal conversion.

The results obtained here stand in contrast to those acquired previously for the naphthalene−nitroxides[1,24,25] and other related compounds;[25] in these studies, direct evidence for enhanced

intersystem crossing was obtained from relative triplet yields acquired from time-resolved absorption spectroscopy.[24,25] The origin of these differences in behavior is not yet clear and will be the subject of future work. Regardless of the precise mechanism, intramolecular quenching of the excited singlet state by the stable nitroxide radicals within these compounds is clearly a highly efficient process with rate constants often exceeding 10^{10} s^{-1} (Table 4).

Acknowledgment. We thank Drs. Steve Atherton and Don O'Connor for their assistance at CFKR, Prof. Daniel Falvey and David Laman for the use of and assistance with the transient absorption system, Armando Herbelin at Western Washington University for molecular modeling work, and Carl Johnson for performing the high resolution mass spectrometry. This work was supported by the ONR (N00014-91-J-1260) and the NIH (1R01GM44966-01A1). Partial support for S. E. Herbelin was provided by a NSF graduate research fellowship. The time-resolved fluorescence measurements were performed at the Center for Fast Kinetics Research, which is supported jointly by the Biomedical Research Technology Program of the Division of Research Resources of the National Institutes of Health (RR00886) and by the University of Texas at Austin.

References and Notes

(1) Green, S. A.; Simpson, D. J.; Zhou, G.; Ho, P. S.; Blough, N. V. *J. Am. Chem. Soc.* **1990,** *122*, 7337 and references therein.

(2) Karpiuk, J.; Grabowski, Z. R. *Chem. Phys. Lett.* **1989,** *160*, 451.

(3) Chattopadhyay, S. K.; Das P. K.; Hug, G. L. *J. Am. Chem. Soc.* **1983,** *105*, 6205.

(4) Yee, W. A.; Kuzmin, V. A.; Kliger, D. S.; Hammond, G. S.; Twarowski, A. J. *J. Am. Chem. Soc.* **1979**, *101*, 5104.

(5) Green, J. A.; Singer, L. A.; Parks, J. H. *J. Chem. Phys.* **1973**, *58*, 2690.

(6) London, E. *Mol. Cell. Biochem.* **1982,** *45*, 181 and references therein.

(7) Yeager, M. D.; Feigenson, G. W. *Biochemistry* **1990**, *29*, 4380.

(8) Matko, J.; Ohki, K.; Edidin, M. *Biochemistry* **1992**, *31*, 703.

(9) Abrams, F. S.; London; E. *Biochemistry* **1992,** *31*, 5312.

(10) Blough, N. V.; Simpson, D. J. *J. Am. Chem. Soc.* **1988,** *110*, 1915.

(11) Kieber, D. J.; Blough, N. V. *Free Radical Res. Commun.* **1990,** *10*, 109.

(12) Kieber, D. J.; Blough, N. V. *Anal. Chem.* **1990,** *62*, 2275.

(13) Kieber, D. J., Johnson, C. G.; Blough, N. V. *Free Radical Res. Commun.* **1992,** *16*, 35.

(14) Johnson, C. G.; Caron, S.; Blough, N. V. *Anal. Chem.* **1996**, *68*, 867.

(15) Blough, N. V.; Zepp, R. G. In *Active Oxygen in Chemistry*; Foote, C. S., Valentine, J. S., Greenberg, A., Liebman, J., Eds.; Chapman and Hall: London, 1995; Chapter 8.

(16) Pou, S.; Huang, Y.-L.; Bhan, A.; Bhadti, V. S.; Hosmane, R. S.; Wu, S. Y.; Cao, G.-L.; Rosen G. M. *Anal. Biochem.* **1993,** *212*, 85.

(17) Li, B.; Gutierrez, P. L.; Blough, N. V. *Anal. Chem.* **1997**, *69*, 4295.

(18) De Bernardo, S.; Weigele, M.; Toome, V.; Manhart, K.; Leimgruber, W.; Bohlen, P.; Stein, S.; Udenfriend, S. *Arch. Biochem. Biophys.* **1974,** *163*, 390.

(19) Weigele, M.; Blount, J. F.; Tengi, J. P.; Czajkowski, R. C.; Leimgruber, W. *J. Am. Chem. Soc.* **1972,** *94*, 4052.

(20) Chandler, R. R.; Coffer, J. L.; Atherton, S. J.; Snowden, P. T. *J. Phys. Chem.* 1992, *96*, 2713.

(21) O'Conner, D. V. *Time Correlated Single Photon Counting*, Academic Press: Orlando, FL, 1984.

(22) Vinter, J. G.; Davies, A.; Saunders: M. R. *J. Comput.-Aided Mol. Design* **1987**, *1*, 31.

(23) Turro, N. J. *Modern Molecular Photochemistry*; University Science Books: Mill Valley, CA, 1991.

(24) Blough, N. V., unpublished observations.

(25) Jenks, W. S. Time-Resolved EPR and Photophysical Studies of the Interactions of Doublet and Triplet States with Stable Nitroxides. Ph.D. Thesis, Columbia University, 1991.